doi:10.1093/brain/awaa116 BRAIN 2020: 143; 1697–1713 | 1697

BRAIN
A JOURNAL OF NEUROLOGY

Nogo receptor decoy promotes recovery and corticospinal growth in non-human primate spinal cord injury

Xingxing Wang,[1,2] Tianna Zhou,[1] George D. Maynard,[3] Pramod S. Terse,[4] William B. Cafferty,[2,5] Jeffery D. Kocsis[2,5] and Stephen M. Strittmatter[1,2,5]

See Bradbury and Oliveira (doi:10.1093/brain/awaa175) for a scientific commentary on this article.

After CNS trauma such as spinal cord injury, the ability of surviving neural elements to sprout axons, reorganize neural networks and support recovery of function is severely restricted, contributing to chronic neurological deficits. Among limitations on neural recovery are myelin-associated inhibitors functioning as ligands for neuronal Nogo receptor 1 (NgR1). A soluble decoy (NgR1-Fc, AXER-204) blocks these ligands and provides a means to promote recovery of function in multiple preclinical rodent models of spinal cord injury. However, the safety and efficacy of this reagent in non-human primate spinal cord injury and its toxicological profile have not been described. Here, we provide evidence that chronic intrathecal and intravenous administration of NgR1-Fc to cynomolgus monkey and to rat are without evident toxicity at doses of 20 mg and greater every other day ($\geqslant$2.0 mg/kg/day), and far greater than the projected human dose. Adult female African green monkeys underwent right C5/6 lateral hemisection with evidence of persistent disuse of the right forelimb during feeding and right hindlimb during locomotion. At 1 month post-injury, the animals were randomized to treatment with vehicle ($n = 6$) or 0.10–0.17 mg/kg/day of NgR1-Fc ($n = 8$) delivered via intrathecal lumbar catheter and osmotic minipump for 4 months. One animal was removed from the study because of surgical complications of the catheter, but no treatment-related adverse events were noted in either group. Animal behaviour was evaluated at 6–7 months post-injury, i.e. 1–2 months after treatment cessation. The use of the impaired forelimb during spontaneous feeding and the impaired hindlimb during locomotion were both significantly greater in the treatment group. Tissue collected at 7–12 months post-injury showed no significant differences in lesion size, fibrotic scar, gliosis or neuroinflammation between groups. Serotoninergic raphespinal fibres below the lesion showed no deficit, with equal density on the lesioned and intact side below the level of the injury in both groups. Corticospinal axons traced from biotin-dextran-amine injections in the left motor cortex were equally labelled across groups and reduced caudal to the injury. The NgR1-Fc group tissue exhibited a significant 2–3-fold increased corticospinal axon density in the cervical cord below the level of the injury relative to the vehicle group. The data show that NgR1-Fc does not have preclinical toxicological issues in healthy animals or safety concerns in spinal cord injury animals. Thus, it presents as a potential therapeutic for spinal cord injury with evidence for behavioural improvement and growth of injured pathways in non-human primate spinal cord injury.

1 Cellular Neuroscience, Neurodegeneration and Repair Program, Yale University School of Medicine, New Haven, CT, USA
2 Department of Neurology, Yale University School of Medicine, New Haven, CT, USA
3 ReNetX Bio, New Haven, CT, USA
4 National Center for Translational Sciences, NIH, Rockville, MD, USA
5 Department of Neuroscience, Yale University School of Medicine, New Haven, CT, USA

Received August 05, 2019. Revised December 19, 2019. Accepted February 23, 2020. Advance access publication May 6, 2020

Correspondence to: Stephen M. Strittmatter
Yale University School of Medicine – Neurology
295 Congress Ave CNNR
BCMM 436 New Haven Connecticut 06536, USA
E-mail: stephen.strittmatter@yale.edu

Correspondence may also be addressed to: Jeffery D. Kocsis
E-mail: jeffery.kocsis@yale.edu

Keywords: axon; regeneration; oligodendrocyte; Nogo receptor; spinal cord injury

Abbreviations: CST = corticospinal tract; NgR1 = Nogo receptor 1; SCI = spinal cord injury

Introduction

Traumatic damage of the spinal cord frequently results in persistent neurological deficits below the level of the injury. The annual incidence of traumatic spinal cord injury (SCI) in the USA exceeds 15 000 and the prevalence of persistent paresis is greater than 300 000 (Lee *et al.*, 2014; GBD 2016 Traumatic Brain Injury and Spinal Cord Injury Collaborators, 2019). Common causes include motor vehicle accidents, military service, falls, sports and gunshot. While neurons are typically lost only at the level of the SCI, symptoms are widespread below level because of the disconnection of surviving neurons in caudal segments from the brain and rostral spinal cord. Therefore, restoring neural networks through axonal growth is key to meaningful neurological recovery. Even for clinically complete SCI, the majority of individuals have remaining tissue bridges though they are not adequate to support function. Neural circuit restoration can therefore occur by axonal sprouting and local reconnectivity of neurons above and below the injury level even when long distance regeneration of individual cut fibres does not occur. This point is highlighted by the ability of caudal stimulation to support limited voluntary movement recovery in otherwise clinically complete SCI cases (Angeli *et al.*, 2018; Gill *et al.*, 2018; Wagner *et al.*, 2018). Despite the fact that limited degrees of axonal sprouting, plasticity or regeneration have the potential to support highly significant recovery of function, there is no FDA approved medical therapy for SCI today.

Cellular and molecular studies over several decades have revealed multiple causes for limited axon growth in the adult CNS. On the one hand, there are cell-autonomous factors that are missing from the adult mammalian CNS, but are present during development and in the adult PNS. These include GAP-43, SPRR1A, KLFs, DLK and calcium channels (Bomze *et al.*, 2001; Bonilla *et al.*, 2002; Hammarlund *et al.*, 2009; Itoh *et al.*, 2009; Moore *et al.*, 2009). Other factors are expressed selectively in adult CNS, and limit axon growth by intrinsic mechanisms, including PTEN and SOCS genes (Liu *et al.*, 2010, 2015; Sekine *et al.*, 2018). Apart from each neuron's expression profile, the environment surrounding the axon is crucial for axon growth, as highlighted by the nerve transplantation studies of Aguyao and colleagues (Richardson *et al.*, 1980; David and Aguayo, 1981). The failure of the adult CNS environment to support axonal growth is due in part to a lack of positive factors such as BDNF, CNTF, IGF1 and other neurotrophins, and extracellular matrix components such as laminin (Schnell *et al.*, 1994; Liu *et al.*, 2002; Byrne *et al.*, 2014; Duan *et al.*, 2015). Perhaps most critically, the adult mammalian CNS contains extracellular inhibitors of axonal growth. The primary source of such inhibitors are glial cells. Reactive astrocytes, as well as neurons, produce chondroitin sulphate proteoglycans (CSPGs), and reactive sprouting is augmented when these molecules are digested with chondroitinase after SCI (Bradbury *et al.*, 2002; Wang *et al.*, 2011*a*; James *et al.*, 2015; Hu *et al.*, 2018; Warren *et al.*, 2018; Rosenzweig *et al.*, 2019). Myelin-forming oligodendrocytes of the CNS are key contributors to the axon growth inhibiting nature of the adult CNS after SCI. These cells produce inhibitory Nogo-A (RTN4A), myelin associated glycoprotein (MAG) and oligodendrocyte myelin glycoprotein (OMgp, encoded by *OMG*), as well as semaphorin 6A and ephrin B3 and CSPGs (McKerracher *et al.*, 1994; Mukhopadhyay *et al.*, 1994; Chen *et al.*, 2000; GrandPre *et al.*, 2000; Kottis *et al.*, 2002; Benson *et al.*, 2005; Runker *et al.*, 2008; Duffy *et al.*, 2012; Shim *et al.*, 2012; Schwab and Strittmatter, 2014).

A range of molecular studies have characterized the action of Nogo-A, MAG and OMgp. These molecules each bind to Nogo-66 receptor 1 (NgR1, encoded by *RTN4R*) (Fournier *et al.*, 2001; Huebner *et al.*, 2011) and also to leucocyte immunoglobulin-like receptor B2 (LILRB2, PirB) (Atwal *et al.*, 2008) and trigger inhibition of anatomical growth in multiple settings, from axon regeneration to sprouting to synaptic plasticity with and without injury (McGee *et al.*, 2005; Akbik *et al.*, 2012, 2013; Schwab and Strittmatter, 2014; Bhagat *et al.*, 2016). Among the inhibitory ligands, Nogo-A appears more critical than MAG or OMgp based on combinatorial gene deletion studies (Cafferty *et al.*, 2010; Lee *et al.*, 2010). While blockade of a single inhibitory molecule can be achieved pharmacologically with a ligand-directed antibody, the multiple ligands and receptors in this pathway implies that no antibody can fully block the system. To overcome this limitation, we developed a soluble decoy receptor, containing the ligand binding domain of NgR1 fused to the Fc portion of IgG1 for protein stability (Li *et al.*, 2004; Wang *et al.*, 2014). The molecule has been optimized to contain alanine substitutions at two cysteine residues to avoid

disulphide scrambling, and the human version is termed NgR1(310)ecto-Fc, or AXER-204.

The ability of intrathecally administered rat NgR1-Fc to promote axonal growth and functional recovery has been demonstrated in multiple models of CNS injury, including thoracic spinal cord dorsal hemisection, spinal contusion injury, dorsal root injury, stroke and glaucoma (Wang *et al.*, 2006, 2011*b*, 2014, 2015). Most critically, the protein is efficacious in chronic contusive SCI when administered long after damage (Wang *et al.*, 2011*b*). The human NgR1-Fc AXER-204 is also effective after bolus lumbar intrathecal dosing in rat SCI and distributes widely in the non-human primate CNS following intrathecal administration (Wang *et al.*, 2014). For these reasons, AXER-204 is entering clinical trials for chronic cervical SCI (ClinicalTrials.gov, NCT03989440).

The current study was designed to provide key support for the clinical development of AXER-204. A crucial issue is safety in multiple species with repeat dosing in healthy and SCI animals. Here, we provide detailed toxicological analysis of AXER-204 safety and report no concerns. Another issue is the demonstration of safety and efficacy in a non-human primate. We randomized African green monkeys 1 month after C5/6 lateral hemisection to receive vehicle or AXER-204 (0.10–0.17 mg/kg/day) continuously by intrathecal lumbar catheter for 4 months. After treatment, motor performance was assessed and the anatomy of injured corticospinal tract (CST) axons determined by anterograde axon tracing. AXER-204 treatment caused no deleterious effects in SCI animals, while promoting functional recovery and CST axon growth caudal to the lesion. These findings provide strong support for clinical testing of AXER-204 in chronic SCI subjects.

Materials and methods

NgR1(310)-Fc decoy protein

The production of human NgR1-Fc decoy receptor (AXER-204) has been described previously, and includes substitution of Ala for Cys at position 266 and 309A of NgR1(Wang *et al.*, 2014). The protein was formulated in sterile phosphate-buffered saline (PBS) at 10 mg/ml and aliquots were stored at −80°C prior to use.

Toxicology studies

Toxicological studies were performed by Covance Nonclincal Safety Assessment Laboratory, Madison, Wisconsin, USA (intrathecal studies in rat and monkey) and IIT Research Institute (IITRI), Chicago, Illinois, USA (intravenous study in rat).

Monkey intrathecal toxicology studies evaluated slow bolus infusions of AXER-204 at three dose levels in comparison to PBS vehicle in male and female cynomolgus monkeys. An initial dose escalation and 14-day range finder study evaluated 30 mg given daily as the top dose with one male and one female per dose group. Subsequently, a GLP intrathecal toxicology study was conducted with 20 mg given every other day as the top dose given for 104 and 108 days in females and males, respectively, followed by a 5-week recovery period. Catheter failures and catheter-related irritation lead to discontinuation of the dosing phase earlier than the planned 180 days. The study included six monkeys/sex/group and three monkeys/sex from each group were assessed for the 5-week recovery period. Assessment of toxicity was based on mortality, clinical observations, body condition scoring, body weight, body weight change, qualitative food consumption, ophthalmic observations, ECG measurements, blood pressure determination, body temperature, respiration rate, heart rate, and clinical and anatomic pathology. Blood samples were collected for toxicokinetic evaluation and anti-drug antibody analysis. CSF samples were collected and analysed for test article content.

C5/C6 right hemisection and intrathecal lumbar catheterization

Adult African green monkeys (vervets, female, baseline body weight 4.2–7.2 kg) were used in the studies and were approved by the Yale Institutional Animal Care and Use Committee. Animals were first anaesthetized with 4% isofluorane and maintained with 2% isofluorane throughout the surgical procedure. Animals were placed in a prone position after anaesthesia. A 5-cm longitudinal skin incision was made at the midline of the neck, and a C5/C6 right hemisection was performed.

After injury, rubber mats were placed in the cage for comfort when lying down and to prevent pressure sores. Animals that could not initially self-feed were fed using a long pair of forceps directly to the mouth. Bowls were placed in the cage and water bottles hung low on the cage. We observed a gradual daily improvement. The animals were able to sit up for short periods of time and self-feed the day after surgery. Buprenorphine was given every 6–12 h for 48 h after surgery. Animals were monitored at least twice a day for the first 5 days then once daily.

Throughout the post-injury period, the animals were checked for appetite including food consumption and water intake. The incision site was monitored to ensure closure and no infection, inflammation or oedema. Movement and general attitude were assessed. In addition, the animals were given a neurological examination initially on weekly then monthly intervals as previously described (Sasaki *et al.*, 2011). Briefly, the state of consciousness, posture, gait in home cage, stimulus and sensation response, extremity and eye movements, as well as hand grasping ability were scored on a point system, with a score of zero corresponding to normal behaviour, and a maximum score of 54 corresponding to severe bilateral neurological impairment. The scoring chart can be found in Supplementary Fig. 1 of Sasaki *et al.* (2011).

One month after SCI, the animals were randomized to treatment group, and were then re-anaesthetized with isoflurane for intrathecal catheter placement. All surgeons, animal handlers, behavioural scorers and histological analysers remained blind to treatment. The first seven animals were randomized 1:1, and the second seven were randomized at a 2:1 ratio of NgR-Fc: Control. A L3–4 laminectomy was performed and an ALZET intrathecal catheter (item# 0007740, DURECT) was implanted into the subdural space at the L3 vertebral level. The catheter was secured to the lumbar muscle with a 4-0 silk suture. The

proximal part of the catheter was routed subcutaneously under the skin of the back to the interscapular area and connected to a mini-osmotic pump (ALZET model 2ML4, DURECT) containing either 2 ml vehicle or Nogo receptor decoy protein [NgR1(310)–Fc]. The 2 ml NgR1(310)-Fc solution contained 20 mg human NgR1(310)-Fc protein providing a dose of 0.10–0.17 mg/kg/day (variation due to different animal body weights). The duration of treatment was 4 months. A new osmotic minipump filled with the same amount of NgR1(310)-Fc or vehicle was replaced once every month.

One animal in the NgR-Fc group had catheter complications at the time of insertion and was euthanized after an unsuccessful attempt at surgical revision. At the time of initial catheter placement several placements were attempted and on the last attempt the wire guideline was kinked and twisted, and there was concern in the operating room for potential root or cord damage. Neurological motor signs (lower limb weakness) were observed immediately after surgery and progressed for several days. The animal was euthanized at 7 days after the catheter implant attempt. Given that the neurological issue was observed immediately after the failed catheter attempt, we considered it an iatrogenic surgical event. None of the other animals had catheter insertion issues and none had additional neurological issues.

Cortical spinal tract tracing

One to two months before sacrifice, animals were re-anaesthetized by inhalation of isofluorane as described earlier. A craniotomy was performed on the left parietal bone. Descending CST fibres were labelled with biotin dextran amine (BDA; molecular weight 10 000; 10% in PBS; Molecular Probes) by injection into 20 spots of left motor cortex anterior to the central sulcus and 1 cm lateral to the midline. Injections were performed using a glass capillary attached to a Hamilton microsyringe, mounted on a micromanipulator using a motorized microinjection drive (PHD Ultra pump; Harvard Apparatus). Each site received two separate injections at depths of 2 mm and 4 mm from the cortical surface. Each injection delivered 300 nl of BDA solution at 100 nl/min. The tip of the glass capillary was left in place for an additional minute before withdrawal. The bone flap was replaced and sealed with tissue fibrin glue (TISSEEL, Baxter) after finishing all cortical injections. All animals were sacrificed 7–16 months after SCI.

Behavioural testing

The behavioural testers were all unaware of the experimental condition (NgR-Fc or vehicle). For open field behavioural assessment, the animals were observed in an observation cage, which was a double housing cage unit (122 cm long × 85 cm high × 66 cm deep) with a clear plexiglass panel inserted on one end for visualization and video recording. The size of the testing cage allowed for study of ambulation with full stride, stepping, and swing movements. Non-surgical animals were able to backflip in this space. During open field assessments, research assistants delivered food to the tops of cages. The animals retrieved the food through cage bars and exhibited feeding behaviour. During the 10-min video analysis, the number of times that the animal used its left, right, or both hands to bring food to its mouth was counted. The hand usage preference was normalized to the control side (left hand, serving as internal control) so that each animal can serve as its own control. For each animal at each time point, the ratio was calculated as (attempts with right hand or both hands) / (all attempts). The pretreatment feeding observation videotape was missing data for one animal later randomized to NgR-Fc. One animal, later randomized to vehicle, continued to use the impaired right forelimb in >80% of episodes at 2 weeks after SCI and prior to randomization, and was excluded from the post-injury analysis for this one post-treatment outcome measure.

Hindlimb motor function in open cage was assessed using video analysis. Assessment rubrics were modified from the literature (Ma *et al.*, 2016). Measures were recorded for each hindlimb of each animal at multiple time points. To perform well on these assessments, the animals had to demonstrate voluntary motor control, which is mediated by corticospinal and rubrospinal systems. Hindlimb movement was scored as follows: no voluntary movement in large joints (hip, knee or ankle) = 0; perceptible movement of one to two joints in the hindlimb = 1; perceptible movement of three joints = 2; vigorous movement of three joints without weight bearing = 3; occasional standing without sustainable weight bearing = 4; consistent weight support = 5. The hindlimb digit function was scored as follows: no bar grasping due to flaccid or spastic digits = 0; attempts digital movement = 1; delay in grasping the bar using digits (palm slips from the bar) = 2; delay in grasping the bar with a slow release or digits of the foot are clumsy while standing = 3; effective movement using digits with rapid shift to a relaxed position as balance is attained, or digits open rapidly to perform the next activity = 4.

Histology and analysis

All histology and image analyses were completed by experimenters without knowledge of treatment group. At the termination of the experiment the animals were given a lethal dose of sodium pentobarbital (100 mg/kg) and perfused through the left cardiac ventricle (right auricle cut) with 1 l cold heparinized saline followed by 1 l of 4% paraformaldehyde. After perfusion brain and spinal cord were removed, post-fixed in 4% formaldehyde at 4°C, and cryoprotected in 30% sucrose. The spinal cord 15 mm rostral to and 15 mm caudal to the lesion was embedded in O.C.T. medium (Sakura Finetek) and cut horizontally at 30 µm thickness on a Leica cryostat. Transverse sections (30-µm thick) were collected from the spinal cord at C1 level and 16 mm to 20 mm caudal to the lesion. The sections were incubated with avidin-biotin-peroxidase complex to detect BDA tracer; anti-5-HT antibody (1:1000; Immunostar), anti-GFAP (1:500; Sigma); anti-Laminin (1:30; Sigma); anti-Collagen IV (1:100; Invitrogen); anti-CD68 (1:500; Bio-Rad); anti-Iba1 (1:250; Wako). The following day after the primary antibody incubation, sections were incubated for 2 h at room temperature with appropriate Alexa 350, Alexa 488, or Alexa 569 secondary antibodies (1:500; Invitrogen). The sections were finally covered with mounting medium (Life Technologies). Images were acquired using a Carl Zeiss LSM 800 confocal microscope. Image processing was performed using Zeiss Zen, ImageJ, and Adobe Photoshop.

For analysis of CST axon regeneration across the lesion site, every sixth consecutive horizontal spinal section (spaced 180 µm apart) was selected. The number of BDA-labelled CST fibres crossing the right/left line at various distance rostral to and

caudal to lesion centre were counted in each section for each animal. For analysis of BDA-CST label efficiency, three transverse spinal sections at C1 level were collected. A confocal image was collected using a Carl Zeiss LSM 800 microscope at ×20 magnification. BDA-labelled axons in three randomly selected boxes (50 × 50 μm) from within this grid were counted. The average numbers from these boxes was then scaled up to total number of axons labelled in the lateral column of the C1 spinal cord white matter. For analysis of CST axon regeneration >12 mm caudal to the lesion site, two transverse spinal sections at the T3–4 level stained for BDA were analysed from each animal and averaged. The length of BDA-labelled fibre in spinal grey matter was measured using confocal *z*-stacks and the ImageJ plugin Axon Tracer (Patel *et al.*, 2018). For analysis of serotonin innervation, immunoreactive serotonin fibres in the ventral horn of transverse sections caudal to the lesion were selected by thresholding. The length of serotonin fibre in the region of interest was measured using the ImageJ plugin Axon Tracer.

For analysis of spinal cord lesion size, consecutive sets of horizontal spinal cord section were stained with anti-GFAP antibody. The length of lesion, the length of spinal cord on lesion side and the length of spinal cord on intact side were measured in each section. In the other consecutive sets of horizontal spinal cord section stained with anti-Laminin antibody, the lesion size with positive laminin staining was measured by using Zeiss Zen software. For one animal in the control group, tissue at the SCI fractured during sectioning, and lesion measurements could not be made.

Statistical analysis

Data were analysed using SPSS or GraphPad Prism software using the specific statistical tests described in the figure legends. All data were included in the analysis, except were indicated above.

Data availability

The data that support the findings of this study are available from the corresponding authors, upon reasonable request.

Results

Toxicological safety of NgR-Fc in non-human primate and rodent

Safety evaluation of AXER-204 included 14-day intrathecal toxicology studies in rat and monkey with daily administration, and pivotal GLP intrathecal toxicology studies in rat with 57 days and monkey with 104–108 days of every other day dosing. No adverse events related to AXER-204 were noted in these studies. For the rat and monkey non-GLP studies, the no-observed-adverse effect level (NOAEL) doses of 1 mg/day and 30 mg/day, respectively, were equal to the maximum doses studied.

The maximum doses studied and the NOAEL doses from the pivotal GLP intrathecal toxicology studies were 1 mg/qad (qad, every other day) and 20 mg/qad for rat and monkey, respectively. Exposure was dose proportional and gender-related differences in exposure were <2-fold within each of the studies.

The pivotal rat intrathecal toxicology study evaluated the toxicity of AXER-204 when given as a repeat dose every other day for up to 2 months followed by a 1-month recovery phase. Male and female rats were administered AXER-204 at 0.15, 0.5, and 1 mg/day every other day for up to 57 days. No AXER-204-related mortalities, clinical observations (effects on body weights, food consumption, ophthalmic observations, or functional observation battery tests), effects on clinical pathology test results, or anatomic pathology findings were noted. Average body weights at the end of the dosing phase for males were 515, 531, 500, and 528 g for vehicle, 0.15, 0.5 and 1 mg/day every other day dose groups, respectively. The corresponding average body weights for females were 316, 316, 320, and 310 g. The between-group differences in average body weight were not statistically significant (one-way ANOVA with Dunnett's). Similarly, AXER-204 did not have an effect on body weight change over the course of the toxicology study. Between-group comparisons of the other toxicological evaluations were likewise unremarkable. Based on these results, the NOAEL for AXER-204 is 1 mg/day.

The pivotal intrathecal toxicology study in monkey was designed to evaluate the toxicity of the test article, AXER-204, when given as a repeat dose every other day for up to 6 months via intrathecal infusion for up to 60 min, to cynomolgus monkeys followed by a 5-week recovery period. Because of catheter-related issues, dosing was modified to 104 days (females) and 108 days (males). Male and female monkeys were administered AXER-204 at 1.92, 10 and 20 mg/day every other day for over 100 days. Administration of AXER-204 did not result in mortality; any abnormal clinical observations; effects on body weight, food consumption, blood pressure determination, body temperature, respiration rate, or heart rate; findings during ECG or ophthalmic examinations or clinical pathology tests; or anatomical pathology findings. Average body weights at the end of the dosing phase for males were 4.5, 4.1, 4.0, and 4.1 kg for vehicle, 1.92, 10 and 20 mg/day every other day dose groups, respectively. The corresponding average body weights for females were 2.7, 3.1, 3.1, and 3.1 kg. The between-group differences in average body weight were not statistically significant (one-way ANOVA and Dunnett's). Similarly, AXER-204 did not have an effect on body weight change over the course of the toxicology study. Between-group comparisons of the other toxicological evaluations were likewise unremarkable. Based on these results, the NOAEL for AXER-204 is 20 mg/day.

Anti-drug antibodies were detected in serum following repeat dose intrathecal administration of AXER-204 in rat and monkey in each of the intrathecal toxicology studies. However, no clear dose-response relationship was identified for the appearance of anti-drug antibodies in the pivotal GLP toxicology studies and there was no clear impact on serum exposure and clearance.

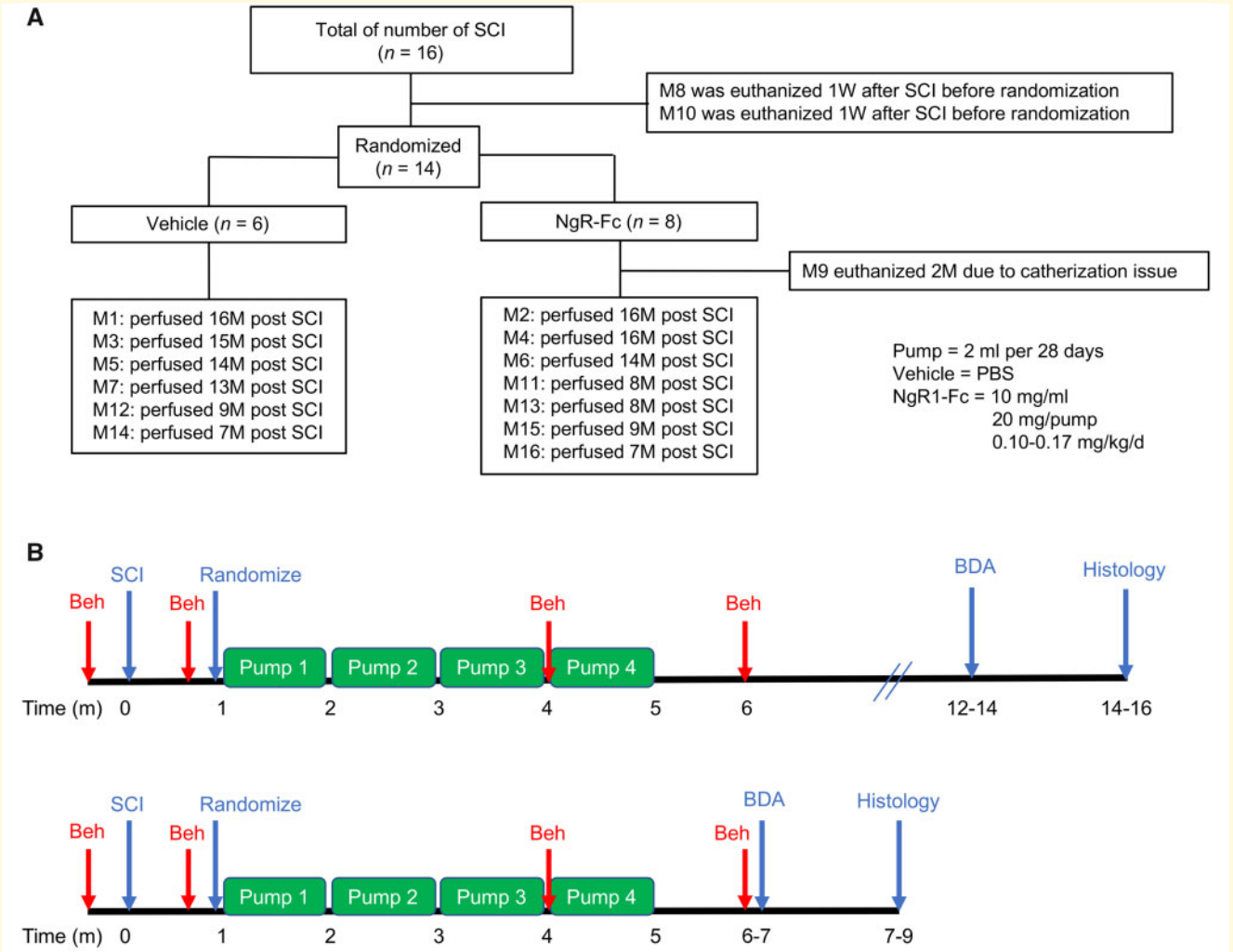

Figure 1 Experimental design. (**A**) Sixteen monkeys received right C5/C6 hemisection spinal cord injury. One week after SCI and prior to randomization, two monkeys were euthanized for humane reasons, because of poor general health. The remaining 14 SCI monkeys were randomly assigned to either the vehicle (PBS)-treated or NgR-Fc-treated groups, and all handlers remained blind to the experimental condition. One monkey from the NgR-Fc-treated group was removed from the experiment 2 months after SCI because of a catheterization issue. Thirteen monkeys completed the experiment and are included in the analysis with six in the vehicle group and seven in the NgR-Fc group. Each NgR-Fc-treated monkey received NgR-Fc protein at 0.10–0.17 mg/kg/day intrathecally for 4 months. (**B**) Schematics of the experiment: two cohorts of animals were studied, seven monkeys in cohort 1. Animals started intrathecal treatment 1 month after SCI and received continuous intrathecal administration with either vehicle ($n = 4$) or NgR-Fc ($n = 3$) for 4 months and were sacrificed 14–16 months after SCI. In cohort 2, six monkeys received the same strategy of intrathecal treatment as cohort 1 with either vehicle ($n = 2$) or NgR-Fc ($n = 4$). Animals were sacrificed 7–9 months after SCI. The timing of SCI, randomization, behavioural studies (Beh), CST axon tracing (BDA) and the four minipump administrations are illustrated.

In addition to the intrathecal toxicology studies, a rat GLP intravenous toxicology study was conducted in order to ensure adequate evaluation for any toxicity that may result due to systemic exposure. The study evaluated a low dose of 0.5 mg/kg/qad and a high dose of 25 mg/kg/qad. There were no AXER-204-related clinical observations (effects on body weights, food consumption, functional observation battery or ophthalmic observations), effects on clinical pathology test results, or anatomical pathology findings noted. Based on these results, the NOAEL for AXER-204 is 25 mg/kg/qad intravenously.

Spinal cord injured non-human primates

We used a right lateral hemisection at C5/6 in African green monkeys to test AXER-204 safety and efficacy. Sixteen female animals were studied (Fig. 1 and Supplementary Table 1). Two animals had complications from the SCI surgery, were euthanized shortly after injury and are not included in the analysis. By 1 month post-injury, the remaining animals were in good overall health, easily moving about their home cage, able to feed freely, and to urinate and defecate without

issue. A subset of animals underwent timed staircase food pellet retrieval tasks and showed timing delays in task completion on the affected side (not shown). At 1 month post-injury the remaining 14 animals were randomized to treatment with vehicle PBS ($n = 6$) or AXER-204 ($n = 8$) (Fig. 1). The dose of AXER-204 was 20 mg protein in 2 ml PBS vehicle infused over 1 month. Given the variable body weights of 4.2–7.2 kg, this yielded 0.10–0.17 mg/kg/day dosing. The infusion was delivered via a lumbar intrathecal cannula placed at the location that would be used for lumbar puncture procedure. Once a month the exhausted subcutaneous minipump was replaced with a fresh pump. One animal in the NgR-Fc group had catheter complications in the first week after placement and was euthanized after an unsuccessful attempt at surgical revision.

The first seven animals were maintained for 6 months after the treatment before tracing CST axons by cortical BDA injection. Because cage-side observations revealed no obvious change from 7 to 12 months in the first cohort, the second cohort of six animals received BDA injections 1 month after the last pump infusion ended (Fig. 1). By cage-side observations of general health, non-excluded animals in both groups remained healthy throughout the experimental period. The general neurological health was monitored by the NeuroScore from 0 (no deficit) to 54 (maximum) (Sasaki *et al.*, 2011). Only minor deficits averaging <5 were observed in either group (Supplementary Fig. 1).

Behavioural outcomes improved by NgR-Fc treatment

Animals were observed in their home cages during eating and walking. To assess forelimb use preference, 48 ± 6 (mean ± standard error of the mean, SEM) feeding episodes for each animal were assessed from 10 min of videotaped observation at each time point. Prior to SCI, animals in both groups used both forelimbs equally (Fig. 2A). The percentage of eating episodes in which the right or both forelimbs were used but not the left forelimb alone was close to 50% in both groups and not significantly different statistically. The same metric was scored at 6 months, 1 month after the fourth month of treatment had ended. The vehicle group ate with the left forelimb alone 94% of the time, revealing a strong SCI-associated disuse of the right forelimb (Fig. 2B). The NgR-Fc treated group exhibited significantly less left-sided preference, using the right affected forelimb in 17% of episodes as opposed 6% in vehicle-treated animals. The time course of improvement for the NgR-Fc group was gradual from pretreatment to 4 months post-injury to 6 months post-injury (Fig. 2C).

Hindlimb performance during walking and climbing in the home cage over 15 min was scored by a blinded observer from videotape using an adaptation of the scale developed by Ma *et al.* (2016). At 6 months post-injury (1 month after last pump infusion), the vehicle group used the hindlimb significantly less effectively than the NgR-Fc treated group ($P = 0.023$, Fig. 2D). The median score of 4 in the NgR-Fc group reflected occasional standing without sustainable weight-bearing, while the median score of 2 in the vehicle group reflects a best performance of perceptible movement of three joints. The hindlimb walking score of individual animals was compared at 1 month post-injury immediately prior to the first treatment with the post-treatment 6-month value. The vehicle animals did not show a significant change during treatment (Fig. 2E), while the NgR-Fc animals improved significantly during treatment ($P = 0.0017$, Fig. 2F). Quantification of hindlimb digit use while standing on a bar was also scored (Fig. 2G). The deficit was less pronounced in the vehicle group for this metric, and the NgR-Fc group showed a trend for better performance. Comparison of hindlimb digit use from 1 month to 6 month post-SCI showed no statistically significant change in the vehicle group (Fig. 2H), but an improvement in the NgR-Fc group ($P = 0.0065$, Fig. 2I). Thus, NgR-Fc infusion from 1 to 5 months improved both forelimb and hindlimb use after cervical SCI.

Lesion size is not altered by delayed NgR-Fc treatment

It is critical to determine if the observed improvements in the NgR-Fc group might be secondary to different lesion sizes between the two groups. At the end of the in-life phase, spinal cord tissue was collected for histological analysis. Sequential horizontal sections were stained with GFAP antibodies and the extent of lesioned versus tissue sparing was determined (Fig. 3A). The percentage to which the hemisection was complete was scored for each animal (Fig. 3G, individual animals in Supplementary Fig. 2) and averaged 85% in both groups with no significant difference. Thus, differences in lesion extent cannot explain the observed behavioural differences, and there is no indication NgR-Fc beginning 1 month post-SCI alters tissue sparing.

Scarring and inflammation are not altered by delayed NgR-Fc treatment

While lesion size was similar in the two groups, the architecture of tissue scarring might also differ between groups and explain behavioural differences. The lesion site was examined at high magnification with regard to GFAP-expressing astrocyte morphology (Fig. 3C–F). Qualitative observation detected no difference in the astrocyte geometry between vehicle and NgR-Fc sections. In the centre of the SCI scar, fibroblasts deposit laminin which persists for months after SCI. We stained alternate sections with anti-laminin antibodies (Fig. 3H–J). Both groups exhibited a central laminin-positive zone and the area of this laminin-expressing area was

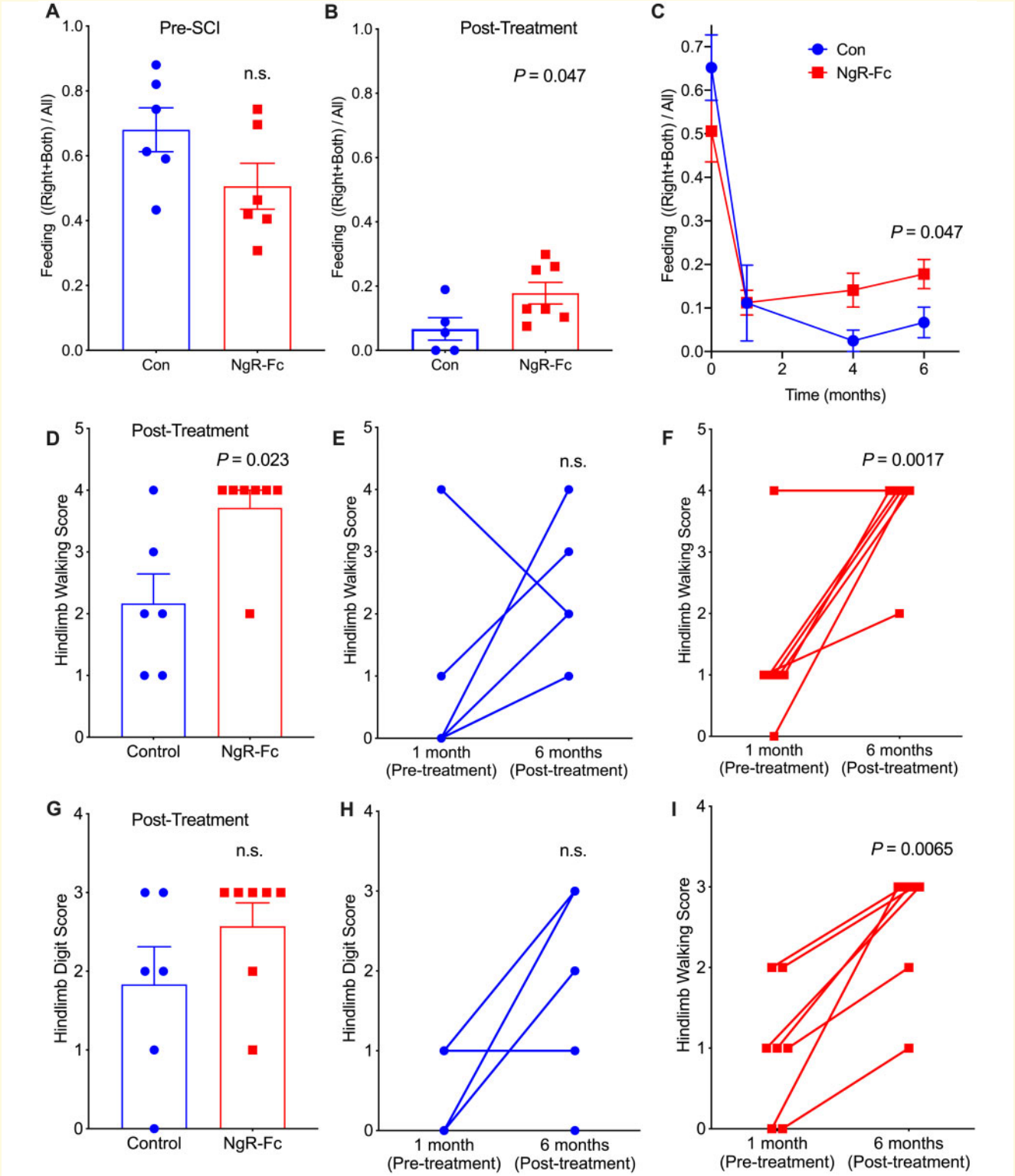

Figure 2 Behavioural recovery of spinal cord-injured monkeys increase by NgR-Fc treatment. (**A**–**C**) Quantifications of open field voluntary feeding behaviour before and 6 months after SCI. (**A**) Hand usage preference 1 week before SCI. In a 10-min video analysis, the number of times that the animal uses its left hand, right hand (lesion side), or both hands to bring food to its mouth was counted. The hand usage preference was normalized to the control side (left hand, serving as internal control). (**B**) Hand usage preference 6 months after SCI. The attempts to use the right hand or both hands increased significantly for animals in the NgR-Fc-treated group ($P = 0.047$ by unpaired two-tailed *t*-test with Welch's correction). Mean ± SEM with individual animals indicated. (**C**) Time course of hand usage preference as a function of time relative to SCI. The pre-injury and 6-month data from **A** and **B** are included in this replot. Mean ± SEM, $n = 6$ for control and $n = 7$ for NgR-Fc. By mixed-effects model, there was a significant interaction of time and treatment, $P = 0.034$, and by unpaired two-tailed *t*-test with Welch's correction at

(continued)

not significantly different between groups. Furthermore, the scarring was similar in groups sacrificed either 12–14 months or 7–9 months after SCI (Supplementary Fig. 3A and B). Thus, the two groups were balanced with respect to scar tissue area and there was no evidence that NgR-Fc treatment from 1 to 5 months post-injury altered chronic scarring.

Damaged SCI tissue is invaded by inflammatory cells and microglia can be detected even in the chronic state. The SCI sections were stained with Iba1 and CD68 markers of resting and activated microglia (Fig. 4A and B). While increased microglial density was detected by both markers around the SCI site even at 7–14 months post-injury, there was no statistically significant difference in area occupied by either marker protein (Fig. 4C and D). Stratification by survival time after SCI did not alter this conclusion (Supplementary Fig. 3C and D). Taken together, the SCI lesions in the two groups were closely matched and no differences in scarring or inflammation between groups were observed.

Raphespinal system intact in control animals

Our hypothesis is that axonal growth after SCI is stimulated by NgR-Fc to account for the improved behaviour, so we sought evidence for axonal growth in the NgR-Fc treated animals. In rodent dorsal hemisection or contusion SCI animals, there is a persistent deficit of raphepsinal fibres below the injury level, and NgR-Fc treatment drives a regenerative sprouting response to partially restore innervation density (Wang *et al.*, 2006, 2011*b*, 2014). Therefore, we stained for raphespinal axon density with an anti-serotonin (5HT) antibody in T1 transverse sections immediately caudal to the cervical cord tissue block. Raphespinal fibres were observed in the intermediolateral column and innervating the ventral horn (Fig. 5A). However, in both the control and NgR-Fc groups, the innervation density in the ventral horn was equal on the right and left sides despite the lateral hemisection (Fig. 5B and C). Thus, a bilateral plexus of raphespinal fibres and spontaneous sprouting in untreated lateral hemisection monkeys prevents any unilateral lesion or asymmetry. The spontaneous recovery of this system prevents an assessment of NgR-Fc action.

Corticospinal axons growth caudal to injury is stimulated by NgR-Fc

The CST pathway contributes to voluntary fine motor function in non-human primate, and shows both sprouting and regenerative responses in rodent SCI in response to NgR-Fc treatment or NgR1 (*RTN4R*) gene deletion. To assess this system in this study we used biotin-dextran-amine injections into the left forelimb motor cortex (affected by the right-sided SCI) at multiple sites. The tracer injections were made after the completion of treatment and behavioural assessments. For the first seven animals the injections were 12–14 months post-injury and in the remainder at 6–7 months post-injury (Fig. 1). To verify the selectivity and robustness of CST labelling after a post-tracer survival period of 1–2 months, we first examined the transverse section well above the injury site and just below the decussation at C1 (Fig. 6). The labelling of the right CST was easily detected in all animals, and counts of total labelled CST fibres per animal yielded an average of ~6000 axons in both experimental groups with no significant differences (Fig. 6D).

Horizontal sections of cervical spinal cord 3 cm in rostro-caudal length centred on the SCI site were examined for the presence of CST fibres from all animals in a blinded fashion. Every sixth section from a consecutive series spanning the entire spinal cord was stained and imaged for CST fibres and counterstained with anti-GFAP antibody to visualize the lesion site. Upon inspection, the rostral segment had intense labelling in all animals (Fig. 7 and additional examples in Supplementary Figs 4–6). Caudal to the injury site, a few CST axons were detected in each animal from the control group (Fig. 7A, D, E, and Supplementary Fig. 6). Caudal CST axons in the NgR-Fc were observed in relative abundance (Fig. 7B, C, F–I and Supplementary Figs 4 and 5). The course of the caudal CST fibres was branched and variable in orientation, and more prominent in grey matter than white matter, consistent with regenerative sprouting. While the abundance of

Figure 2 Continued

6 months, $P = 0.047$ for treatment as in **B**. (**D–I**) Hindlimb functional recovery after NgR-Fc treatment. (**D**) In the open field video analysis of movement assay, hip, knee and ankle movements were scored 6 months after SCI. The NgR-Fc treatment group shows significant recovery of their joint's movements in the hindlimb walking assessment ($P = 0.023$ by unpaired two-tailed *t*-test with Welch's correction). (**E** and **F**) Comparison of hindlimb walking scores at 1 week pre-injury and 6 months post-injury for each individual monkey. There was a statistically significant difference for animals from the NgR-Fc treatment group ($P = 0.0017$ by unpaired two-tailed *t*-test with Bonferroni-Dunn correction for multiple tests) and no significant difference for animals from the vehicle treatment group ($P = 0.07$). Mean ± SEM with individual animals indicated. (**G**) Quantification of the hindlimb digital function. There was a trend of increasing hindlimb digital scores in the NgR-Fc-treated group compared to the vehicle-treated group, but no significant statistical difference. (**H** and **I**) Comparison of hindlimb digital function scores at 1 week pre-injury and 6 months post-injury for each individual monkey. There was a statistically significant difference for animals from the NgR-Fc treatment group ($P = 0.0065$ by unpaired two-tailed *t*-test with Bonferroni-Dunn correction for multiple tests) and no significant difference for animals from the vehicle treatment group ($P = 0.07$). Mean ± SEM with individual animals indicated.

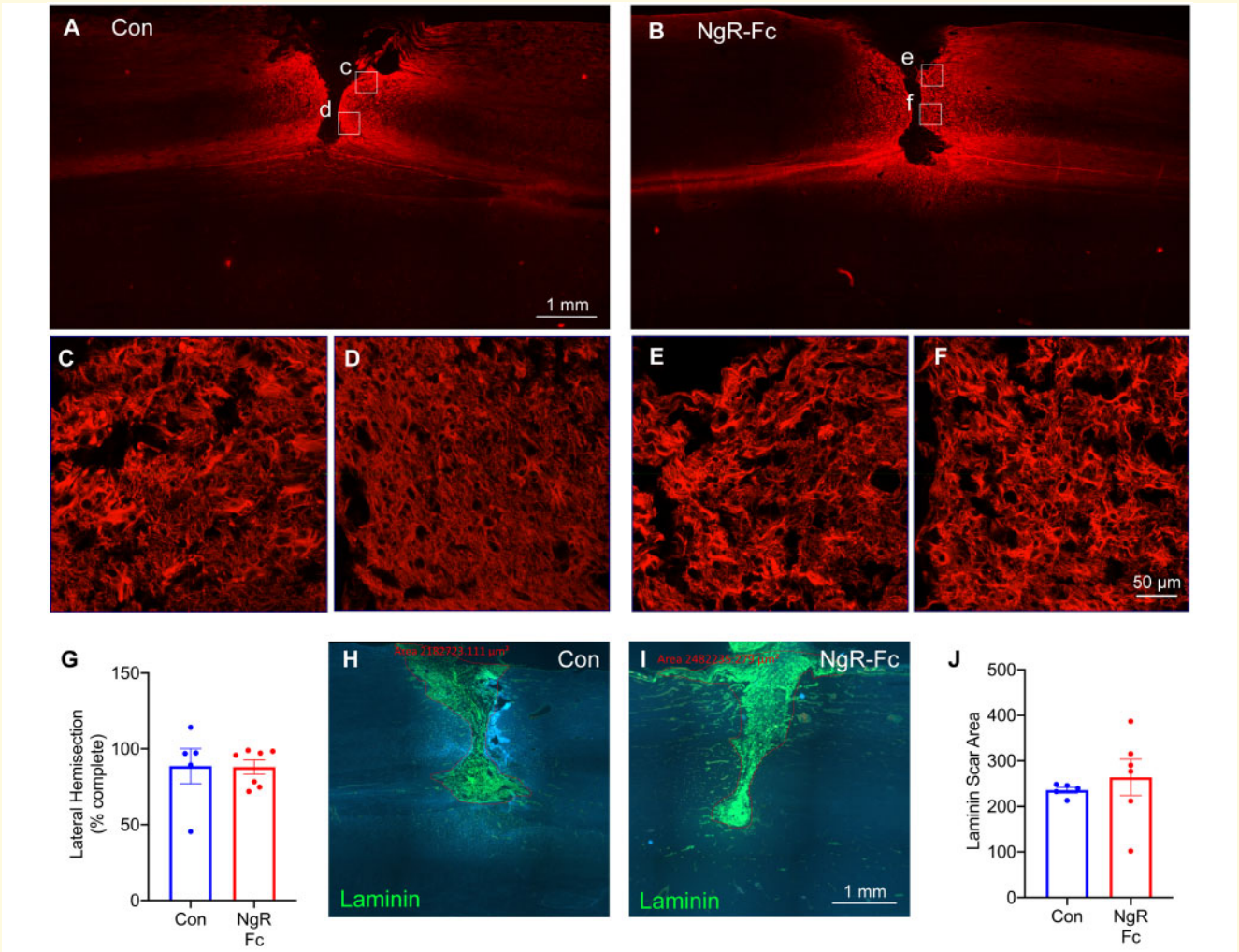

Figure 3 Lesion size is similar in the vehicle and NgR-Fc groups. (**A** and **B**) Representative images of horizontal section of the lesion segment of spinal cord from both the PBS-treated (**A**) and NgR-Fc-treated (**B**) animals, stained with anti-GFAP antibody to visualize the injury site. Rostral is to the *left* and right side is *up*. Scale bar = 1000 μm. (**C**–**F**) Boxed areas in **A** and **B** are magnified in **C**–**F**. Scale bar = 50 μm. (**G**) The depth of lesion at the injury site was measured for each consecutive GFAP stained section. Mean ± SEM with individual animals indicated. There was no statistically significant difference between the two treatment groups. (**H** and **I**) Representative images of the horizontal section of the lesion segment of spinal cord from PBS- (**H**) and NgR-Fc-treated (**I**) animals, stained with anti-Laminin antibody to show the fibrotic scar. Red outlines indicate the fibrotic area. Scale bar = 1000 μm. (**J**) Quantification of the laminin-positive fibrotic scar area. There was no statistically significant difference between groups. Data are mean ± SEM, unpaired two-tailed *t*-test.

CST fibre growth NgR-Fc group, the pattern did not appear to differ between groups.

We counted all CST fibres at 1 mm incremental rostral-caudal positions in each of the stained sections spanning the lesion and normalized to the fibre count 1.5 cm rostral to the SCI site (Fig. 8). Caudal to the lesion, the number of CST fibres was significantly greater in the NgR-Fc group (Fig. 8A, repeated measures ANOVA $P = 0.006$). At a distance of 12 mm caudal to the lesion, the axon index for control animals was 4 ± 1, which corresponds to ∼240 CST axons, while in NgR-Fc-treated animals the value was over twice as great, 10 ± 1.5, or ∼600 CST axons (Fig. 8B, $P < 0.01$). To evaluate the location of CST axons in caudal sections, we averaged counts for 7–12 mm caudal to the injury summed from all depths of the spinal cord (Fig. 8C). The averaged counts confirmed the significant differences between groups from the individual position counts ($P = 0.00018$). Separating the counts between the intact side and the injured side, showed that more fibres were present on the uncrossed intact side, opposite to the rostral CST injury. The NgR-Fc-induced increase of intact side CST axons caudal to the injury was significantly greater than control ($P = 0.0059$). The NgR-Fc-induced increase for cohorts with 12–14 months versus 7–9 months survival post-SCI was indistinguishable (Supplementary Fig. 7), indicating that fibre growth occurring during the treatment period was maintained for 5 months after NgR-Fc treatment ceased.

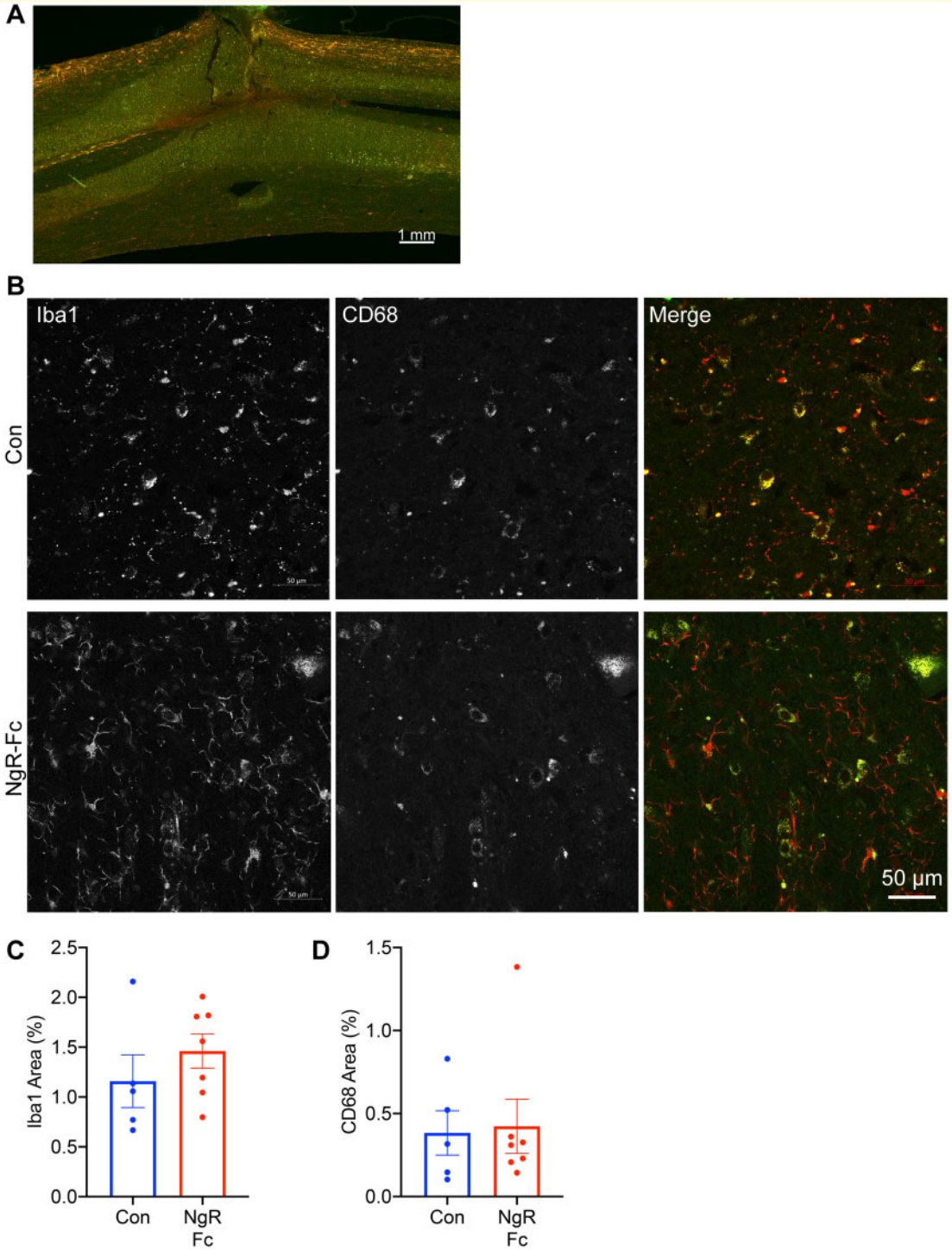

Figure 4 NgR-Fc treatment does not alter chronic gliosis. (**A**) Representative image of immunofluorescent staining for Iba1 (green) and CD68 (red) in horizontal spinal cord sections containing the SCI site. Scale bar = 500 µm. (**B**) High-magnification view near the lesion area stained as in **A** from a vehicle-treated animal (Con) and a NgR-Fc-treated animal (NgR-Fc). Scale bar = 50 µm. (**C** and **D**) Quantification of Iba1 and CD68 immunoreactive area from sections, as in **A** and **B**. There was no statistically significant difference between groups. Data are mean ± SEM, unpaired two-tailed *t*-test.

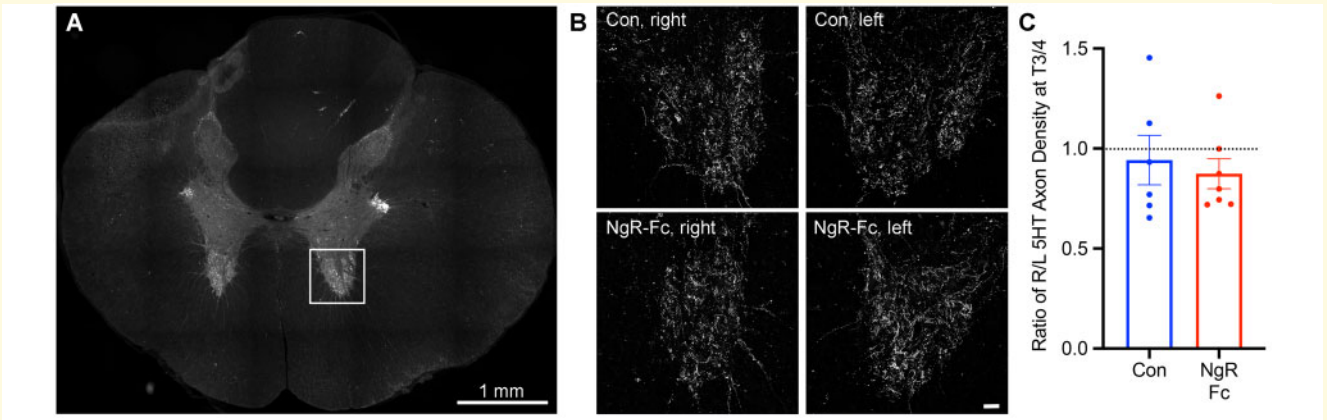

Figure 5 Intact raphespinal serotonergic innervation of the caudal spinal cord after injury. (**A**) Representative low-magnification transverse section of the spinal cord caudal to the lesion site at the T3-T4 level stained with anti-serotonin antibody with the ventral horn measurement area indicated by white square. Scale bar = 1000 μm. (**B**) 5HT fibres in the ventral horn from sections stained, as in **A**, are from a vehicle or NgR-Fc sample of the ventral horn on the right side or left side, as indicated. Scale bar = 50 μm. (**C**) The ratio of 5HT axon length per area in the ventral horn of the lesion side to the intact side was measured for sections as in **B**. There was no statistically significant difference of raphespinal serotonergic innervation between left and right, or between two treatment groups. Data are mean ± SEM, unpaired two-tailed *t*-test.

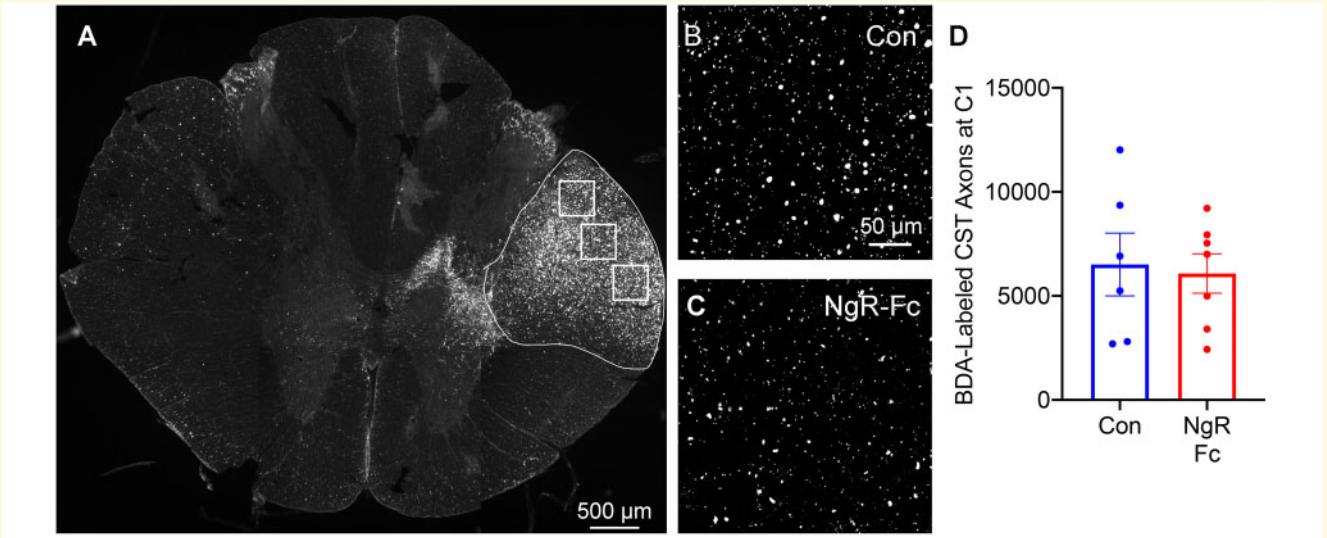

Figure 6 Efficiency of BDA tracing in CST. (**A**) A transverse section of spinal cord at the C1 level was stained for BDA-labelled CST fibres. Three high-magnification images from the regions shown by white boxes were used for quantification of total density in right dorso-lateral CST outlined in white. Scale bar = 500 μm. (**B** and **C**) Representative of high-magnification images of BDA-labelled CST axons in the right lateral column at C1 level from a vehicle-treated animal (**B**) and a NgR-Fc-treated animal (**C**). Scale bar = 50 μm. (**D**) Quantification of BDA-labelled CST axons at C1 spinal cord. No statistically significant difference between groups. Data are mean ± SEM, unpaired two-tailed *t*-test.

Analysis of more caudal transverse sections of spinal cord at T3–4 for CST fibres also revealed a statistically significant increase of grey matter axon length in the NgR-Fc treated group ($P = 0.013$), with a statistically significant NgR-Fc-induced increase on both the lesion side ($P = 0.022$) and the intact side ($P = 0.00085$) (Fig. 8D). The absolute magnitude of CST axon length in the horizontal plane was greater on the lesion side than the intact side, suggesting greater ramification of CST fibres in the denervated grey matter. Overall, NgR-Fc treatment during the period from 1 to 5 months post-SCI increases caudal CST fibre number below the lateral cervical hemisection.

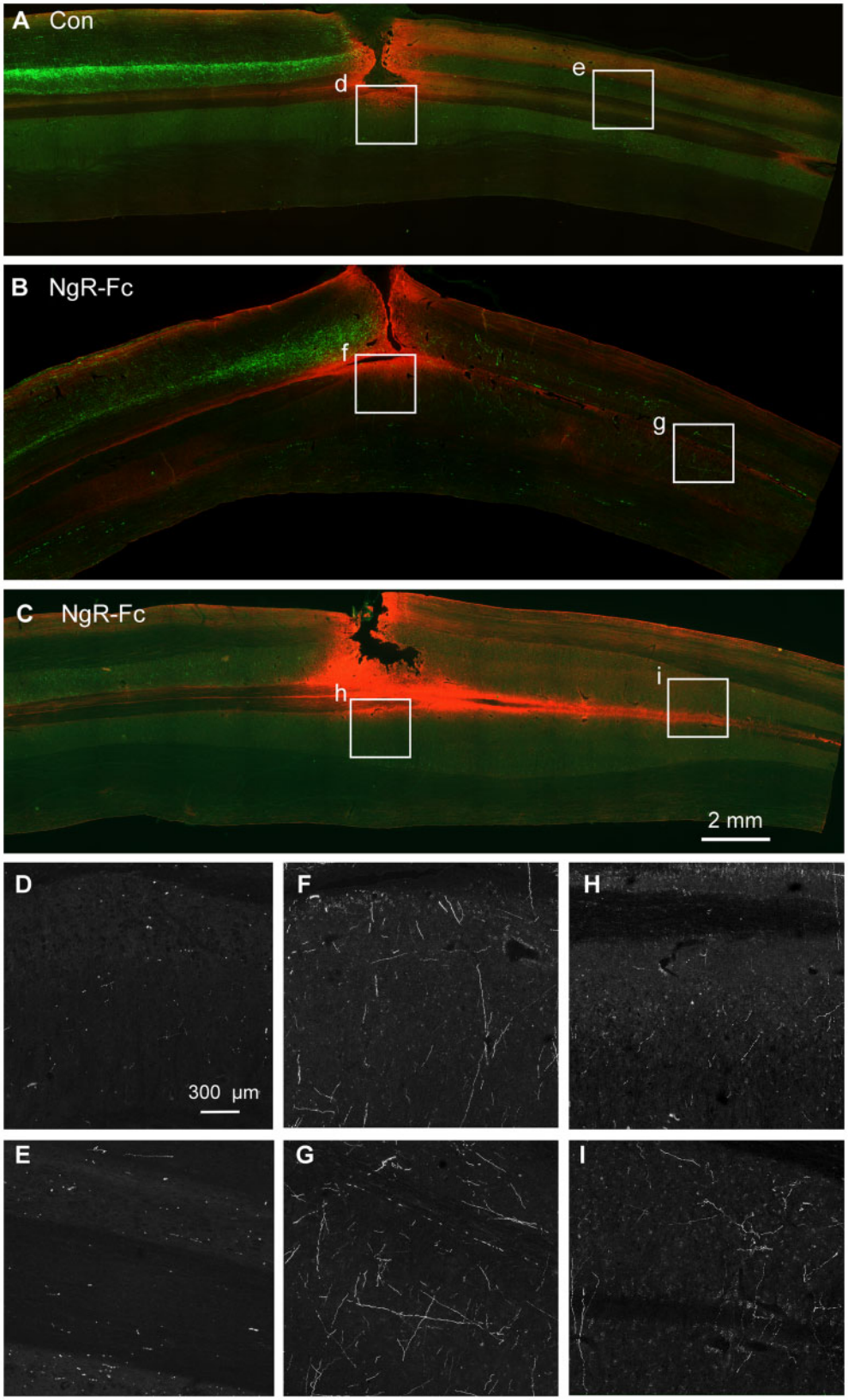

Figure 7 NgR-Fc treatment increases growth of CST fibres caudal to the injury. Representative images of horizontal section of spinal cord stained for BDA (green) and anti-GFAP (red) from one vehicle-treated (**A**) and two NgR-Fc-treated animals (**B** and **C**). Rostral to the *left* and right side is *up*. The area in the white boxes from **A**–**C** (marked **d**–**i**) are magnified in **D**–**I**. Note numerous BDA-labelled CST fibres significantly increased in the NgR-Fc treated animals. Scale bar = 2000 μm in **A**–**C**, 300 μm in **D**–**I.**

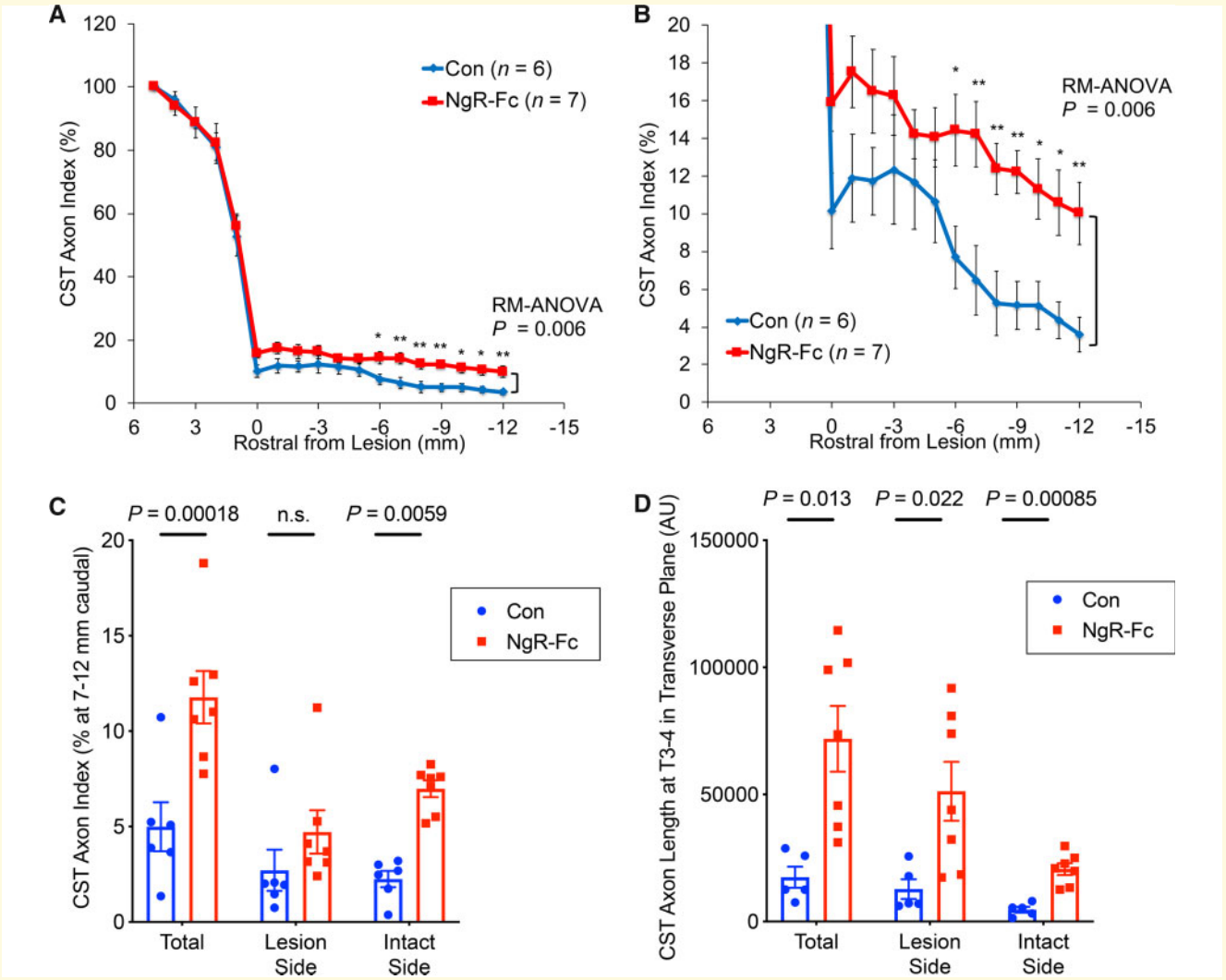

Figure 8 Quantification of BDA-labelled CST axons. (**A**) CST fibre counts from horizontal sections, as in Fig. 7, are reported by an axon index relative to the most rostral count, and are plotted as a function of rostral-caudal distance relative to the SCI site. Repeated measures ANOVA caudal to the lesion show a significant greater fibre count ($P = 0.006$) in the NgR-Fc group, with *post hoc* pairwise comparisons at the indicated distances $^{*}P < 0.05$; $^{**}P < 0.01$. Data are mean ± SEM. (**B**) Enlarged view of graph from **A** from the lesion centre to 12 mm caudal to the injury. (**C**) The average CST axon index from 7–12 mm caudal to the injury on the lesion side, on the intact side and on both sides of the spinal cord. There was statistically greater CST fibre density in the NgR-C group overall, and on the intact side. Unpaired two-tailed *t*-test with Holm-Sidak correction for multiple comparisons. Mean ± SEM, with individual animals indicated. (**D**) Transverse sections of the spinal cord caudal to the lesion site at the T3-T4 level were stained for BDA-labelled CST fibres. The CST axon length per area in the grey matter of the lesion side and the intact side was measured for control (Con) and NgR-Fc groups. Unpaired two-tailed *t*-test with Holm-Sidak correction for multiple comparisons. Mean ± SEM, with individual animals indicated.

Discussion

The main findings of the present study are the safety of intrathecal NgR-Fc (AXER-204) and its efficacy to enhance functional recovery and axon growth in non-human primate. Extended toxicological studies revealed no safety concerns in rat for either the intrathecal and intravenous routes, and in monkey for repeated intrathecal administration. Moreover, at therapeutic doses the compound had no ill effects for spinal injured monkeys. After lateral cervical hemisection, NgR-Fc treatment was efficacious to improve behavioural performance and to promote fibre growth caudal to the lesion. Thus, the current studies provide key support for clinical testing of AXER-204 for recovery of function in chronic SCI.

The toxicological studies explored two routes of repeated administration in two species. Rats received repeated intrathecal dosing for 2 months at dosing rates ~20-fold greater than those previously determined to be efficacious for recovery from SCI, and intravenous dosing for 1 month at rates ~400-fold greater than efficacious. Cynomologus monkeys received repeated intrathecal dosing for 104–108 days at dosing rates ~10-fold greater than those determined to be efficacious for recovery from SCI in rat and here, in non-

human primate SCI. No safety concerns were identified in any of these animals related to AXER-204. The current study also administered the efficacious dose of 0.10–0.17 mg/kg/day intrathecally to African green monkeys with SCI for 4 months and cage-side observations revealed no safety concerns. Thus, the data documented the preclinical safety of repeated intrathecal NgR-Fc administration.

NgR-Fc is hypothesized to promote axonal growth and functional recovery by blocking the activity of Nogo, MAG and OMgp (Akbik *et al.*, 2013; Schwab and Strittmatter, 2014). As such, it is not anticipated to alter scarring, lesion size or microglial responses. Indeed, when the AXER-204 administration began 1 month after injury and tissue was examined 6–12 months later, none of these features were altered. It remains possible that use of NgR-Fc in the acute or subacute period might alter one of these parameters at least transiently. We conclude that NgR-Fc does not alter the generalized tissue reaction to SCI in the non-human primate model used here.

Behavioural observations revealed that the administration of NgR-Fc improved neurological function. Control animals rarely use the affected limb for feeding while the AXER-204 did so three times more frequently. Notably, this improvement is for a task contributing to the animal's daily routine in their home cage and not a specifically trained task. Improvement was not limited to the forelimb, and use of the affected hindlimb was significantly greater for the NgR-Fc group compared to their post-SCI, pretreatment baseline and also compared to the control group. Thus, with an extended delay after lateral cervical hemisection, treatment with AXER-204 improved use and performance of the affected side.

The hypothesis derived from molecular studies and prior rodent SCI work is that the behavioural improvement is due to NgR-Fc release of axon growth. In this injury model, the raphespinal fibre system showed no laterality below the injury in control monkeys. Presumably, this is due to the high level of endogenous plasticity in this system and its extensive bilateral innervation. In this setting, NgR-Fc did not create any evidence of aberrant overgrowth, but its ability to augment endogenous plasticity could not be assessed. With more severe and bilateral injuries, the raphespinal system might be critical for limited recovery and more relevant to study.

Our characterization of axonal anatomy focused on the descending CST. The CST has been highlighted as being particularly relevant for primate motor recovery, both human and non-human (Friedli *et al.*, 2015). This tract was robustly labelled with anterograde tracer and fibres were clearly visible in the caudal spinal cord. There was highly significant increase in fibre density to 250% of control SCI group levels after NgR-Fc treatment. Of note, these measurements were made months after the NgR-Fc infusion ended and therefore reflect a persistent increase. A greater fibre increase is observed on the intact side than the injured side caudally, suggesting that sprouting of uncrossed and uninjured CST fibres play a major role. In these chronically injured African green monkeys, the density of CST fibres for the control group was low but detectable, ~5% of fibre density rostral to the lesion. This persistence of a low CST fibre count is more pronounced than observed previously (Friedli *et al.*, 2015), and may be due to more complete lesions, or the horizontal as opposed to transverse plane of section or to the different non-human primate species. Regardless, it is clear that NgR-Fc treatment increases both axonal growth caudal to the injury site and functional recovery after SCI in these monkeys.

While we observed a significant increase in behavioural recovery and anatomical plasticity, there are limitations to this study. The anatomical evidence for NgR-Fc-induced caudal CST axon growth is correlated with greater behavioural function, but the causative role of this axon sprouting for function is not demonstrated. It remains possible that sprouting of other fibre systems in the spinal cord and brain contribute significantly, and the structural plasticity of synapses as well as axon extension play a role. Studies in rodents suggest that all of the mechanisms can be increased by NgR1 loss of function. Another limitation relates to the dose administered. Only a single dose level based on rodent studies was used, so it is unclear if lower levels would be equally effective or if higher levels would yield further benefit. In addition, intended clinical use of AXER-204 will employ repeated bolus administration, but here we used continuous minipump infusion to simply the experimental design. The two regimens are equally effective in the rodent (Wang *et al.*, 2014).

Overall, the current results provide crucial support for clinical testing of AXER-204. First and foremost, repeated dosing at high levels is safe over time in different species and routes of administration in both healthy and SCI animals. Of note, safety testing with anti-Nogo antibodies has been demonstrated to be well tolerated in human phase 1 studies (Kucher *et al.*, 2018). In addition, the results show that efficacy of NgR-Fc extends from rodent to non-human primates. Thus, preclinical studies show that the AXER-204 safely increases axonal growth in the injured spinal cord with enhanced neurological function.

Funding

This work was supported by NCI-Leidos Contract No. HHSN261200800001E under the BrIDGS/NCATS Program, by the Department of Veterans Affairs BLR&D and RR&D Services (I01 BX003190; B9260-L) to J.D.K., and by grants from the N.I.H. (R35 NS097283) and the Falk Medical Research Trust to S.M.S. at Yale.

Competing interests

S.M.S. is a founder and equity holder and G.M. is an employee and equity holder in ReNetX Bio, Inc. which seeks clinical development of AXER-204. ReNetX Bio is now sponsoring a clinical trial to examine AXER-204 safety and efficacy in chronic cervical spinal cord injury.

Supplementary material

Supplementary material is available at *Brain* online.

References

Akbik F, Cafferty WBJ, Strittmatter SM. Myelin associated inhibitors: a link between injury-induced and experience-dependent plasticity. Exp Neurol 2012; 235: 43–52.

Akbik FV, Bhagat SM, Patel PR, Cafferty WB, Strittmatter SM. Anatomical plasticity of adult brain is titrated by Nogo Receptor 1. Neuron 2013; 77: 859–66.

Angeli CA, Boakye M, Morton RA, Vogt J, Benton K, Chen Y, et al. Recovery of over-ground walking after chronic motor complete spinal cord injury. N Engl J Med 2018; 379: 1244–50.

Atwal JK, Pinkston-Gosse J, Syken J, Stawicki S, Wu Y, Shatz C, et al. PirB is a functional receptor for myelin inhibitors of axonal regeneration. Science 2008; 322: 967–70.

Benson MD, Romero MI, Lush ME, Lu QR, Henkemeyer M, Parada LF. Ephrin-B3 is a myelin-based inhibitor of neurite outgrowth. Proc Natl Acad Sci USA 2005; 102: 10694–9.

Bhagat SM, Butler SS, Taylor JR, McEwen BS, Strittmatter SM. Erasure of fear memories is prevented by Nogo Receptor 1 in adulthood. Mol Psychiatry 2016; 21: 1281–9.

Bomze HM, Bulsara KR, Iskandar BJ, Caroni P, Skene JH. Spinal axon regeneration evoked by replacing two growth cone proteins in adult neurons. Nat Neurosci 2001; 4: 38–43.

Bonilla IE, Tanabe K, Strittmatter SM. Small proline-rich repeat protein 1A is expressed by axotomized neurons and promotes axonal outgrowth. J Neurosci 2002; 22: 1303–15.

Bradbury EJ, Moon LD, Popat RJ, King VR, Bennett GS, Patel PN, et al. Chondroitinase ABC promotes functional recovery after spinal cord injury. Nature 2002; 416: 636–40.

Byrne AB, Walradt T, Gardner KE, Hubbert A, Reinke V, Hammarlund M. Insulin/IGF1 signaling inhibits age-dependent axon regeneration. Neuron 2014; 81: 561–73.

Cafferty WB, Duffy P, Huebner E, Strittmatter SM. MAG and OMgp synergize with Nogo-A to restrict axonal growth and neurological recovery after spinal cord trauma. J Neurosci 2010; 30: 6825–37.

Chen MS, Huber AB, van der Haar ME, Frank M, Schnell L, Spillmann AA, et al. Nogo-A is a myelin-associated neurite outgrowth inhibitor and an antigen for monoclonal antibody IN-1. Nature 2000; 403: 434–9.

David S, Aguayo A. Axonal elongation into peripheral nervous system "bridges" after central nervous system injury in adult rats. Science 1981; 214: 931–3.

Duan X, Qiao M, Bei F, Kim IJ, He Z, Sanes JR. Subtype-specific regeneration of retinal ganglion cells following axotomy: effects of osteopontin and mTOR signaling. Neuron 2015; 85: 1244–56.

Duffy P, Wang X, Siegel CS, Tu N, Henkemeyer M, Cafferty WB, et al. Myelin-derived ephrinB3 restricts axonal regeneration and recovery after adult CNS injury. Proc Natl Acad Sci USA 2012; 109: 5063–8.

Fournier AE, GrandPre T, Strittmatter SM. Identification of a receptor mediating Nogo-66 inhibition of axonal regeneration. Nature 2001; 409: 341–6.

Friedli L, Rosenzweig ES, Barraud Q, Schubert M, Dominici N, Awai L, et al. Pronounced species divergence in corticospinal tract reorganization and functional recovery after lateralized spinal cord injury favors primates. Sci Transl Med 2015; 7: 302ra134.

GBD 2016 Traumatic Brain Injury and Spinal Cord Injury Collaborators. Global, regional, and national burden of traumatic brain injury and spinal cord injury, 1990-2016: a systematic analysis for the Global Burden of Disease Study 2016. Lancet Neurol 2019; 18: 56–87.

Gill ML, Grahn PJ, Calvert JS, Linde MB, Lavrov IA, Strommen JA, et al. Neuromodulation of lumbosacral spinal networks enables independent stepping after complete paraplegia. Nat Med 2018; 24: 1677–82.

GrandPre T, Nakamura F, Vartanian T, Strittmatter SM. Identification of the Nogo inhibitor of axon regeneration as a Reticulon protein. Nature 2000; 403: 439–44.

Hammarlund M, Nix P, Hauth L, Jorgensen EM, Bastiani M. Axon regeneration requires a conserved MAP kinase pathway. Science 2009; 323: 802–6.

Hu HZ, Granger N, Pai SB, Bellamkonda RV, Jeffery ND. Therapeutic efficacy of microtube-embedded chondroitinase ABC in a canine clinical model of spinal cord injury. Brain 2018; 141: 1017–27.

Huebner EA, Kim BG, Duffy PJ, Brown RH, Strittmatter SM. A multidomain fragment of Nogo-A protein is a potent inhibitor of cortical axon regeneration via Nogo receptor 1. J Biol Chem 2011; 286: 18026–36.

Itoh A, Horiuchi M, Bannerman P, Pleasure D, Itoh T. Impaired regenerative response of primary sensory neurons in ZPK/DLK gene-trap mice. Biochem Biophys Res Commun 2009; 383: 258–62.

James ND, Shea J, Muir EM, Verhaagen J, Schneider BL, Bradbury EJ. Chondroitinase gene therapy improves upper limb function following cervical contusion injury. Exp Neurol 2015; 271: 131–5.

Kottis V, Thibault P, Mikol D, Xiao Z-C, Zhang R, Dergham P, et al. Oligodendrocyte-myelin glycoprotein (OMG) is an inhibitor of neurite outgrowth. J Neurochem 2002; 82: 1566–9.

Kucher K, Johns D, Maier D, Abel R, Badke A, Baron H, et al. First-in-man intrathecal application of neurite growth-promoting anti-Nogo-A antibodies in acute spinal cord injury. Neurorehabil Neural Repair 2018; 32: 578–89.

Lee BB, Cripps RA, Fitzharris M, Wing PC. The global map for traumatic spinal cord injury epidemiology: update 2011, global incidence rate. Spinal Cord 2014; 52: 110–6.

Lee JK, Geoffroy CG, Chan AF, Tolentino KE, Crawford MJ, Leal MA, et al. Assessing spinal axon regeneration and sprouting in Nogo-, MAG-, and OMG-deficient mice. Neuron 2010; 66: 663–70.

Li S, Liu BP, Budel S, Li M, Ji B, Walus L, et al. Blockade of Nogo-66, myelin-associated glycoprotein, and oligodendrocyte myelin glycoprotein by soluble Nogo-66 receptor promotes axonal sprouting and recovery after spinal injury. J Neurosci 2004; 24: 10511–20.

Liu K, Lu Y, Lee JK, Samara R, Willenberg R, Sears-Kraxberger I, et al. PTEN deletion enhances the regenerative ability of adult corticospinal neurons. Nat Neurosci 2010; 13: 1075–81.

Liu X, Williams PR, He Z. SOCS3: a common target for neuronal protection and axon regeneration after spinal cord injury. Exp Neurol 2015; 263: 364–7.

Liu Y, Himes BT, Murray M, Tessler A, Fischer I. Grafts of BDNF-producing fibroblasts rescue axotomized rubrospinal neurons and prevent their atrophy. Exp Neurol 2002; 178: 150–64.

Ma Z, Zhang YP, Liu W, Yan G, Li Y, Shields LBE, et al. A controlled spinal cord contusion for the rhesus macaque monkey. Exp Neurol 2016; 279: 261–73.

McGee AW, Yang Y, Fischer QS, Daw NW, Strittmatter SM. Experience-driven plasticity of visual cortex limited by myelin and Nogo receptor. Science 2005; 309: 2222–6.

McKerracher L, David S, Jackson DL, Kottis V, Dunn RJ, Braun PE. Identification of myelin-associated glycoprotein as a major myelin-derived inhibitor of neurite growth. Neuron 1994; 13: 805–11.

Moore DL, Blackmore MG, Hu Y, Kaestner KH, Bixby JL, Lemmon VP, et al. KLF family members regulate intrinsic axon regeneration ability. Science 2009; 326: 298–301.

Mukhopadhyay G, Doherty P, Walsh FS, Crocker PR, Filbin MT. A novel role for myelin-associated glycoprotein as an inhibitor of axonal regeneration. Neuron 1994; 13: 757–67.

Patel A, Li Z, Canete P, Strobl H, Dulin J, Kadoya K, et al. AxonTracer: a novel ImageJ plugin for automated quantification of axon regeneration in spinal cord tissue. BMC Neurosci 2018; 19: 8.

Richardson PM, McGuinness UM, Aguayo AJ. Axons from CNS neurons regenerate into PNS grafts. Nature 1980; 284: 264–5.

Rosenzweig ES, Salegio EA, Liang JJ, Weber JL, Weinholtz CA, Brock JH, et al. Chondroitinase improves anatomical and functional outcomes after primate spinal cord injury. Nat Neurosci 2019; 22: 1269–75.

Runker AE, Little GE, Suto F, Fujisawa H, Mitchell KJ. Semaphorin-6A controls guidance of corticospinal tract axons at multiple choice points. Neural Dev 2008; 3: 34.

Sasaki M, Honmou O, Radtke C, Kocsis JD. Development of a middle cerebral artery occlusion model in the nonhuman primate and a safety study of i.v. infusion of human mesenchymal stem cells. PLoS One 2011; 6: e26577.

Schnell L, Schneider R, Kolbeck R, Barde YA, Schwab ME. Neurotrophin-3 enhances sprouting of corticospinal tract during development and after adult spinal cord lesion. Nature 1994; 367: 170–3.

Schwab ME, Strittmatter SM. Nogo limits neural plasticity and recovery from injury. Curr Opin Neurobiol 2014; 27: 53–60.

Sekine Y, Lin-Moore A, Chenette DM, Wang X, Jiang Z, Cafferty WB, et al. Functional genome-wide screen identifies pathways restricting central nervous system axonal regeneration. Cell Rep 2018; 23: 415–28.

Shim SO, Cafferty WB, Schmidt EC, Kim BG, Fujisawa H, Strittmatter SM. PlexinA2 limits recovery from corticospinal axotomy by mediating oligodendrocyte-derived Sema6A growth inhibition. Mol Cell Neurosci 2012; 50: 193–200.

Wang D, Ichiyama RM, Zhao R, Andrews MR, Fawcett JW. Chondroitinase combined with rehabilitation promotes recovery of forelimb function in rats with chronic spinal cord injury. J Neurosci 2011a; 31: 9332–44.

Wang X, Baughman KW, Basso DM, Strittmatter SM. Delayed Nogo receptor therapy improves recovery from spinal cord contusion. Ann Neurol 2006; 60: 540–9.

Wang X, Duffy P, McGee AW, Hasan O, Gould G, Tu N, et al. Recovery from chronic spinal cord contusion after Nogo receptor intervention. Ann Neurol 2011b; 70: 805–21.

Wang X, Lin J, Arzeno A, Choi JY, Boccio J, Frieden E, et al. Intravitreal delivery of human NgR-Fc decoy protein regenerates axons after optic nerve crush and protects ganglion cells in glaucoma models. Invest Ophthalmol Vis Sci 2015; 56: 1357–66.

Wang X, Yigitkanli K, Kim CY, Sekine-Komo T, Wirak D, Frieden E, et al. Human NgR-Fc decoy protein via lumbar intrathecal bolus administration enhances recovery from rat spinal cord contusion. J Neurotrauma 2014; 31: 1955–66.

Wagner FB, Mignardot JB, Le Goff-Mignardot CG, Demesmaeker R, Komi S, Capogrosso M, et al. Targeted neurotechnology restores walking in humans with spinal cord injury. Nature 2018; 563: 65–71.

Warren PM, Steiger SC, Dick TE, MacFarlane PM, Alilain WJ, Silver J. Rapid and robust restoration of breathing long after spinal cord injury. Nat Commun 2018; 9: 4843.